



Prediction of fouling resistance and permeate flux in cross-flow micellar-enhanced ultrafiltration (MEUF)

Jin-Hui Huang^{a,b,*}, Shao-Hui Guo^{a,b}, Guang-Ming Zeng^{a,b,*}, Ya-Lan Xiong^{a,b}, Dong-Mei Zhang^{a,b}, Xiao-Jiao Tang^{a,b}, Geng-Xin Xie^{a,b}

^a College of Environmental Science and Engineering, Hunan University, Changsha 410082, PR China

^b Key Laboratory of Environmental Biology and Pollution Control (Hunan University), Ministry of Education, Changsha 410082, PR China

ARTICLE INFO

Article history:

Received 20 November 2011
Received in revised form 7 March 2012
Accepted 13 March 2012
Available online 21 March 2012

Keywords:

Model
Permeate flux
Fouling resistance
Cross-flow
MEUF

ABSTRACT

Cross-flow micellar-enhanced ultrafiltration had been used to separate pollutants from waste water effectively, while permeate flux decline with time because of the increase of fouling resistance. According to resistances in series theory, total transport resistance is the sum of two parts: membrane hydrodynamic resistance and fouling resistance. By observing material balance and hydrodynamic type of filtration, we proposed an analysis method of fouling resistance that was based on cross-flow filtration and took into account the presence of micelles instead of traditional cake resistance theory that was built from dead-end filtration. We found permeate flux decline not only by the relationship of time $t^{1/2}$ that traditional cake resistance theory said, but also by concentration of fouling layer ϕ (or φ). Retentate non-recycled and retentate recycled cross-flow experiments were carried out under different operate conditions (i.e., transmembrane pressure (*TMP*) and initial concentration) by using artificial cadmium (Cd) contaminated water and sodium dodecyl sulfate (SDS) and models showed excellent accuracy to predict permeate flux through correlation r^2 from 0.935 to 0.990.

© 2012 Elsevier B.V. All rights reserved.

1. Introduction

Micellar-enhanced ultrafiltration (MEUF) is widely used in separating pollutants from aqueous stream today, including the removal of organic and inorganic solids and various anions and cations [1–6]. Studies have shown its effectivity in mechanical filter process for the unique separation capabilities and low pressure [7–16]. Fig. 1 describes a schematic of a two components counterion-surfactant system in cross-flow MEUF. The metal ions are absorbed in the surfactant micelles surface directly by electrostatic interaction which is the primary binding power in MEUF [17–19]. Simultaneously, charged cadmium ions bridged surfactant micelles which make micelles easily to get together. The surfactant micelles whose sizes are larger than the pore sizes of ultrafiltration membrane are retained by membrane and metal ions on the surface of micelles are removed. However, due to the attachment of micelles to membrane surface, more serious fouling layer was formed in MEUF process than that of general ultrafiltration (UF) [20]. Although this fouling layer plays a certain role in filtering the solution

and improves the efficiency of filtration to a certain extent, it causes serious increase in fouling resistance and permeate flux decline. Besides of mechanical filtration, MEUF has its unique characteristics, including solubilization, micellization and adsorption of micelles. Therefore, modeling of fouling resistance and permeate flux in cross-flow MEUF cannot be described with the model of general cross-flow UF [20]. It is an important and complex research topic in membrane separation process [21–24].

Various models have been developed to predict permeate flux in MEUF. Purkait et al. [23] built the model of gel layer thickness in cross-flow MEUF using hexadecyl (cetyl) pyridinium chloride as the cationic surfactant. But the formula of gel layer resistance which they cited was built based on dead-line filtration process. Rahmanian et al. [24] used fuzzy logic to simulate lead removal and permeate flux in MEUF based on Box–Behnken design (BBD). Fuzzy logic has its advantages that it provides a simple and easy approach to describe the relationships between operational conditions and permeate flux. However, it lacks of intuitive. Danis et al. [22] used a model to investigate the performance of MEUF. Although the model could describe the phenomenon of flux decline in MEUF to a certain extent, it was cited from a centrifugation-ultrafiltration system [25]. Das et al. [21] used localized adsorption model to predict permeate flux in cross-flow MEUF. They built a bridge between gel layer concentration and feed counterion concentration through experimental data fitting while this bridge did not undergo

* Corresponding authors at: College of Environmental Science and Engineering, Hunan University, Changsha 410082, PR China. Tel.: +86 731 88821413; fax: +86 731 88821413.

E-mail address: huangjinhui.59@163.com (J.-H. Huang).

Nomenclature

a	specific surface of micelle (m^2/m^3)
A	area of membrane (m^2)
b	flux model constant in Eq. (12) (s^2/m^2)
b'	flux model constant in Eq. (19) (s^2/m^2)
c	flux model constant in Eq. (12) ($\text{m s}/\text{kg}$)
c'	flux model constant in Eq. (19) ($\text{m s}/\text{kg}$)
C_0	initial feed concentration (kg/m^3)
C_c	retentate concentration of retentate non-recycled system (kg/m^3)
C_p	permeate concentration (kg/m^3)
C_r	feed concentration of retentate recycled system (kg/m^3)
C_0^{Cd}	feed Cd concentration (kg/m^3)
C_0^{SDS}	feed SDS concentration (kg/m^3)
CMC	critical micelle concentration (kg/m^3)
f	condensed degree of feed in retentate non-recycled system
J	permeate flux ($\text{m}^3/\text{m}^2 \text{ s}$)
J_1	permeate flux in retentate non-recycled system ($\text{m}^3/\text{m}^2 \text{ s}$)
J_2	permeate flux in retentate recycled system ($\text{m}^3/\text{m}^2 \text{ s}$)
L	fouling layer thickness (m)
Re	Reynolds number
R_f	fouling resistance (m^{-1})
R_{f1}	fouling resistance in retentate non-recycled system (m^{-1})
R_{f2}	fouling resistance in retentate recycled system (m^{-1})
R_m	membrane hydrodynamic resistance (m^{-1})
t	filtration time (s)
TMP	transmembrane pressure (Pa)
V	permeate volume (m^3)
V_0	total volume in batch cell (m^3)
V_c	retentate volume (m^3)
V_f	filtration volume of the feed (m^3)
w	return rate in retentate recycled system

Greek symbols

α	specific fouling resistance (m/kg)
ε	fouling layer porosity
v	linear velocity based on filter area (m/s)
μ	dynamic viscosity of the solution (Pa s)
ρ_f	density of fouling layer (kg/m^3)
ϕ	concentration of fouling layer in retentate non-recycle cross-flow (kg/m^3)
φ	concentration of fouling layer in retentate recycle cross-flow (kg/m^3)

theoretical derivation or study verification. Therefore, modeling of fouling resistance and permeate flux in cross-flow MEUF is very urgent and meaningful.

In the present study, Due to traditional cake resistance model [20] was derived from dead-line material balance, we proposed an analysis method of fouling resistance by establishing cross-flow material balance and took into account the presence of micelles. Then, using resistances in series theory [20] and mathematic calculus, model of permeate flux in cross-flow MEUF was built. We found permeate flux decline not only by the relationship of time that traditional cake resistance model said, but also the concentration of fouling layer. Therefore, model parameters ϕ (or φ), which integrated from initial concentration and operate conditions, was

introduced to describe the concentration of fouling layer. Cross-flow filtration has two types generally: (i) retentate non-recycled that is the retentate solution does not back to feed tank for filtering again and (ii) retentate recycled. Experiments were conducted to verify the models at various conditions (feed concentration, TMP , types of cross-flow, time) and the results were also collated and analyzed. In the present study, two types cross-flow permeate flux were predicted and analyzed from the perspective of fouling resistance.

2. Theory

2.1. The ideas of building a permeate flux decline model

Some assumptions are presented as the premise of models. (i) In MEUF, Cd^{2+} ions in the solution were trapped in the electric field of micelle and moved with the micelles. These ions were no longer osmotically active [5,26,27]. Therefore, osmotic pressure is ignored. (ii) The shape of micelle varies not only with the structure of the hydrophilic head group, but also with changes in the electrolyte content, temperature, pH, and the presence of additives in the solution [28]. With 30°C , $\text{pH} = 7$, aqueous media, the shape of SDS micelle can be considered as typical spherical under low critical micelle concentration (CMC).

The relationship between permeate flux and transmembrane pressure (TMP) was bridged through laminar Blake–Kozeny equation. Therefore, fluid type of MEUF must be determined at first by using Reynolds number. Material balance of cross-flow was used to eliminate the variable (thickness of fouling layer) of laminar Blake–Kozeny equation. In addition, different types of cross-flow had different material balance. Then, equations of fouling resistance in retentate recycled and non-recycled cross-flow MEUF were found respectively by laminar Blake–Kozeny equation and material balance. Naturally, models of permeate flux were found by using resistances in series theory and mathematics calculus.

2.2. Modeling of permeate flux decline

2.2.1. Retentate non-recycled system

According to the definition of permeate flux [29] and resistances in series model [20]. Equation of permeate flux is obtained:

$$J = \frac{1}{A} \frac{dV}{dt} = \frac{TMP}{\mu(R_m + R_f)} \quad (1)$$

where J is permeate flux ($\text{m}^3/\text{m}^2 \text{ s}$), A is area of membrane (m^2), V is permeate volume (m^3), t is filtration time (s), TMP is transmembrane pressure (Pa), μ is dynamic viscosity of solution (Pa s), R_m is membrane hydrodynamic resistance (m^{-1}), R_f is fouling resistance (m^{-1}).

With the operational condition of experiment, Reynolds number $Re = \rho u_0 d / \mu$, where, u_0 is average velocity in channel, d is diameter of cross-flow channel, and ρ , μ are solution density and dynamic viscosity, respectively. With the operating TMP (60, 100, 150 kPa), the Reynolds number for all the operating velocity (0.026, 0.032, 0.040 m/s) is far less than 2000. Therefore, hydrodynamic type of MEUF is laminar flow. For laminar flow, the deduced laminar Blake–Kozeny equation [29,30] is showed to apply to filtration:

$$\frac{TMP}{L} = \frac{5\mu v(1-\varepsilon)^2 a^2}{\varepsilon^3} \quad (2)$$

where L is fouling layer thickness (m), ε is fouling layer porosity, a is specific surface of micelle (m^2/m^3), v is linear velocity based on filter area (m/s), μ is dynamic viscosity of solution (Pa s). For typical spherical SDS micelle, specific surface $a = 6/d_s$, d_s is diameter of micelle (m) and diameter of typical spherical SDS micelle is 4 nm

[31]. Linear velocity v , is based on the empty cross-sectional area and

$$v = \frac{dV/dt}{A} \quad (3)$$

A material balance is needed to establish a link between Eqs. (2) and (3) in retentate non-recycled system and given:

$$C_0V_f = LA(1 - \varepsilon)\rho_f + C_cV_c + C_pV \quad (4)$$

where C_0 is initial concentration in feed (kg/m^3), unchanged with filtration, V_f is volume of feed which has been filtered (m^3), and it finally equals the total volume of batch cell, ρ_f is density of fouling layer (kg/m^3), C_c is retentate concentration, V_c is retentate volume (m^3), and C_p is permeate concentration.

In Eq. (4), $V_c = V_f - V - \varepsilon LA$ and εLA is volume of filtrate held in fouling layer. The calculated value of L is about 10^{-3} to 10^{-4} m by equation: $R_f = \text{specific fouling resistance } \alpha \times L$. Moreover, εLA turns out to be about 0.1–1% of volume of feed. Therefore, the volume of filtrate held in fouling layer is insignificance and neglected [29]. Define $f = V/V_f$, and f represents condensed degree of feed. It is controlled by using the retentate back valve and keeps unchanged with filtration. Then, Eq. (4) becomes:

$$C_0V = fLA(1 - \varepsilon)\rho_f + C_c(1 - f)V + fC_pV \quad (5)$$

Substituting Eq. (3) into Eq. (2) and using Eq. (5) to eliminate L , a final equation is obtained as:

$$\begin{aligned} \frac{dV}{Adt} &= \frac{TMP}{\mu(5(1 - \varepsilon)a^2/\rho_f\varepsilon^3)((C_0 - C_c(1 - f) - C_p f)V/fA)} \\ &= \frac{TMP}{\mu(\alpha(C_0 - C_c(1 - f) - C_p f)V/fA)} \end{aligned} \quad (6)$$

where α is specific fouling resistance (m/kg), and defined as:

$$\alpha = \frac{5(1 - \varepsilon)a^2}{\rho_f\varepsilon^3} \quad (7)$$

According to resistances in series theory, transport resistance in filtrating process includes two main contributions: (i) R_m , membrane hydrodynamic resistance, constant in time, which is related to the properties of membrane. (ii) R_f , fouling resistance. Therefore, Eq. (6) indicates the expression of fouling resistance in retentate non-recycled system:

$$R_{f1} = \frac{\alpha(C_0 - C_c(1 - f) - C_p f)V}{fA} \quad (8)$$

where R_{f1} is fouling resistance in retentate non-recycled system (m^{-1}). To simplify the equation, we define $\phi = (C_0 - C_c(1 - f) - C_p f)/f$, and ϕ is introduced to depict the integrated result of each parts, represented the concentration of fouling layer, and then Eq. (8) becomes:

$$R_{f1} = \frac{\alpha\phi V}{A} \quad (9)$$

Using Eqs. (9) and (1), Eq. (1) can be integrated to obtain an expression of permeate volume versus time in retentate non-recycled system as:

$$V = \frac{-\mu R_m + (\mu^2 R_m^2 + 2\mu\alpha\phi TMPt)^{1/2}}{\mu\alpha\phi/A} \quad (10)$$

Substituting Eq. (10) into Eq. (9) to eliminate V , a function of fouling resistance in retentate non-recycled system is obtained:

$$R_{f1} = \left(R_m^2 + \frac{2\alpha TMP}{\mu} \phi t \right)^{1/2} - R_m = \frac{TMP}{\mu} (b + c\phi t)^{1/2} - R_m \quad (11)$$

where b, c are constant parameters in retentate non-recycled MEUF, $b = \mu^2 R_m^2 / TMP^2$, $c = 2\alpha\mu / TMP$. Integrating Eq. (10) with initial condition: $t = 0, V = 0$, a function of permeate flux in retentate non-recycled system is obtained:

$$J_1 = \left(\frac{\mu^2 R_m^2}{TMP^2} + \frac{2\alpha\mu}{TMP} \phi t \right)^{-1/2} = (b + c\phi t)^{-1/2} \quad (12)$$

where J_1 is permeate flux in retentate non-recycled system ($\text{m}^3/\text{m}^2 \text{ s}$).

2.2.2. Retentate recycled system

Similarly, a material balance was given in retentate recycled system:

$$C_0V_0 = LA(1 - \varepsilon)\rho_f + C_r(V_0 - V) + C_pV \quad (13)$$

where V_0 is total volume in batch cell (m^3), C_0 is initial concentration in feed. However, retentate solution is recycled to feed tank and C_r becomes feed concentration. Define $w = V/V_0$, and w represents return rate. It changes with the volume of permeate. Then, Eq. (13) becomes:

$$C_0V = wLA(1 - \varepsilon)\rho_f + C_r(1 - w)V + wC_pV \quad (14)$$

Similarly, substituting Eq. (3) into Eq. (2) and using Eq. (14) to eliminate L , expression of fouling resistance in retentate recycled system is obtained:

$$R_{f2} = \frac{\alpha(C_0 - C_r(1 - w) - C_p w)V}{wA} \quad (15)$$

where R_{f2} is fouling resistance in retentate recycled system (m^{-1}). In retentate recycled system, we proposed a model parameter $\varphi = (C_0 - C_r(1 - w) - C_p w)/w$, and φ represents the concentration of fouling layer. Then, Eq. (15) becomes:

$$R_{f2} = \frac{\alpha\varphi V}{A} \quad (16)$$

From Eqs. (16) and (1), permeate volume in retentate recycled system can be expressed as a function of time:

$$V = \frac{-\mu R_m + (\mu^2 R_m^2 + 2\mu\alpha\varphi TMPt)^{1/2}}{\mu\alpha\varphi/A} \quad (17)$$

Substituting Eq. (17) into Eq. (16) to eliminate V , a function of fouling resistance in retentate recycled system is obtained:

$$R_{f2} = \left(R_m^2 + \frac{2\alpha TMP}{\mu} \varphi t \right)^{1/2} - R_m = \frac{TMP}{\mu} (b' + c'\varphi t)^{1/2} - R_m \quad (18)$$

where b', c' are constant parameters in retentate recycled MEUF, $b' = \mu^2 R_m^2 / TMP^2$, $c' = 2\alpha\mu / TMP$. Integrating Eq. (17) with initial condition $t = 0, V = 0$, an equation of permeate flux of time in retentate recycled system is obtained:

$$J_2 = \left(\frac{\mu^2 R_m^2}{TMP^2} + \frac{2\alpha\mu}{TMP} \varphi t \right)^{-1/2} = (b' + c'\varphi t)^{-1/2} \quad (19)$$

where J_2 is permeate flux in retentate recycled system.

Prediction of parameters ϕ and φ , representing concentration of fouling layer, were mentioned in Section 4.3. Parameters b, c, b', c' in Eqs. (12) and (19) are obtained by fitting the calculated curve using Origin software. The value of specific fouling resistance and membrane hydrodynamic resistance are determined in filtration experiments by methods mentioned in Sections 4.1 and 4.2.

Eqs. (11), (12), (18) and (19) are built to simulate fouling resistance and permeate flux intuitively in cross-flow MEUF. Each parameter in those equations has its significance and represents specific operate factor. Taken advantage of this, specific operate factor could be obtained by observing intercept or slope of related graph. We can also control the filtration process through adjusting

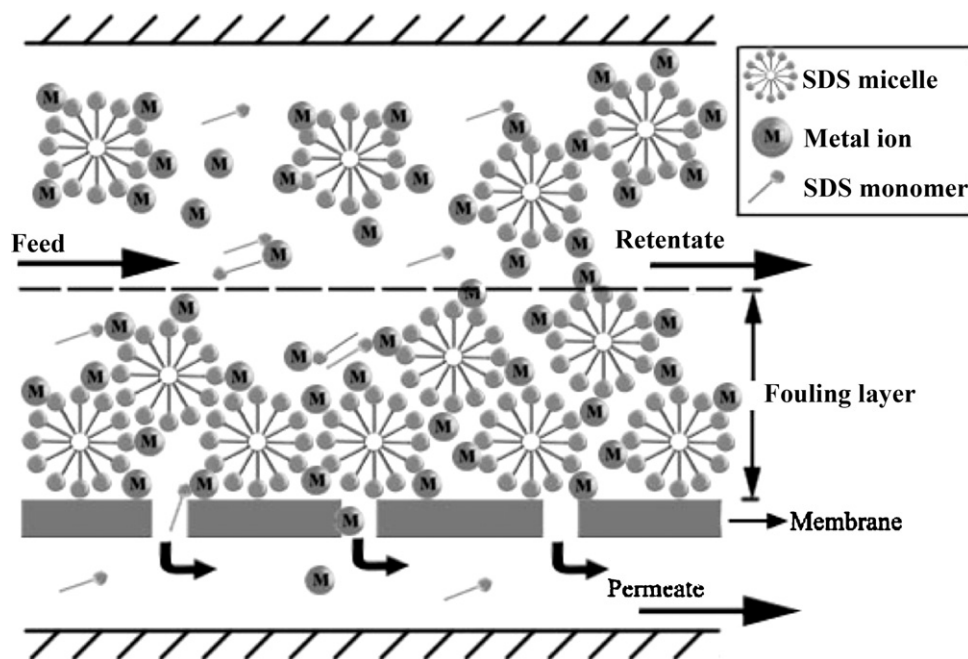


Fig. 1. A schematic diagram of separation of metal ions by MEUF using SDS micelles.

specific operate factor and find the most suitable operate conditions. The method of model derivation can be extended to other membrane filtration processes. From Eqs. (11) and (18), the mathematical significance of fouling resistance versus ϕt or φt indicates a parabola. From Eqs. (12) and (19), permeate flux versus ϕt or φt indicates an exponential decline curve.

3. Experiment

3.1. Materials

The chemicals used are as follows: Sodium dodecyl sulfate (SDS) ($C_{12}H_{25}NaSO_4$, MW 288.38, AR, 1 CMC = 2.2494 kg/m³ [4]) was obtained from Tianjin Kermel Chemical Reagents Development Center, China. Cadmium nitrate tetrahydrate ($Cd(NO_3)_2 \cdot 4H_2O$, MW 308.48, AR) was obtained from Shanghai Tingxin Chemical Reagent Company, China. Sodium hydroxide (NaOH, MW 40, AR) was purchased from Sinopharm chemical reagent company, China. The deionized water used in all experiments was produced from a water purification system (type 90007-03) purchased from Lab-conco, USA.

3.2. Ultrafiltration unit

An improved composite biomax membranes of MWCO 10,000 Da, obtained from Pellicon XL Device, Millipore Corporation, USA. The characteristics of membrane are: pH operating range, 2–14; operating temperature, 4–50 °C; maximum operating pressure, 5.6 bar; filtration area, 50 cm².

MEUF system is modified from Millipore LabScale™ TFF System for meeting the requirements of feed tank. Set-up of the system is shown in Fig. 2.

From 10 L feed tank, feed solution is pumped through a cross-flow filtration cell to two lines A or B. A, retentate non-recycled, represents the line that retentate solution do not back to feed tank after filtration. B, retentate recycled, represents the line that retentate solution back to feed tank after filtration. The desired TMP in filtration cell is shown by pressure gauge and controlled by feed pump and retentate back pressure valve.

3.3. Experiment procedure

The cross-flow MEUF experiments were carried out in batch cell with two types: (i) the line of retentate non-recycled, described as A line in Fig. 2 (ii) the line of retentate recycled, described as the line of B in Fig. 2. Selected TMP was 60 kPa, 100 kPa, 150 kPa, while SDS concentration was controlled at 4 CMC. For all experiments, feed cadmium ions concentration was kept constant at 100 mg/L. SDS concentrations were selected at 1 CMC, 2 CMC, 4 CMC, while TMP was controlled at 100 kPa. Due to the low concentration of metal ion compared with that of surfactant concentration, SDS concentration was defined to solution concentration. Diluted HNO₃ and NaOH for pH adjustment of solutions in experiments were used and pH was adjusted to 7.0. All the experiments were conducted at 30 ± 2 °C maintained by stirring hot plate.

Before using a fresh membrane, membrane was washed by distilled water at the pressure of 100 kPa for 30 min. The pure water permeate flux at various TMP were measured by flowmeter and permeability of membrane was determined by the curve slope of flux versus TMP. And membrane hydrodynamic resistance is obtained

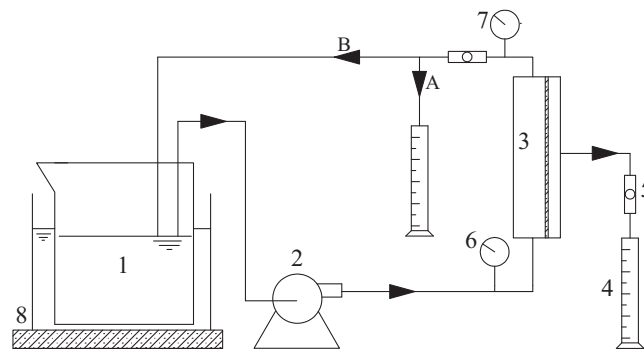


Fig. 2. Experimental set-up of batch cross-flow MEUF unit: 1, feed tank; 2, feed pump; 3, membrane filtration unit; 4, measuring cylinder; 5, flowmeter; 6, feed pressure gauge (in); 7, retentate pressure gauge (out); 8, stirring hot plate; A, retentate non-recycled line; B, retentate recycled line.

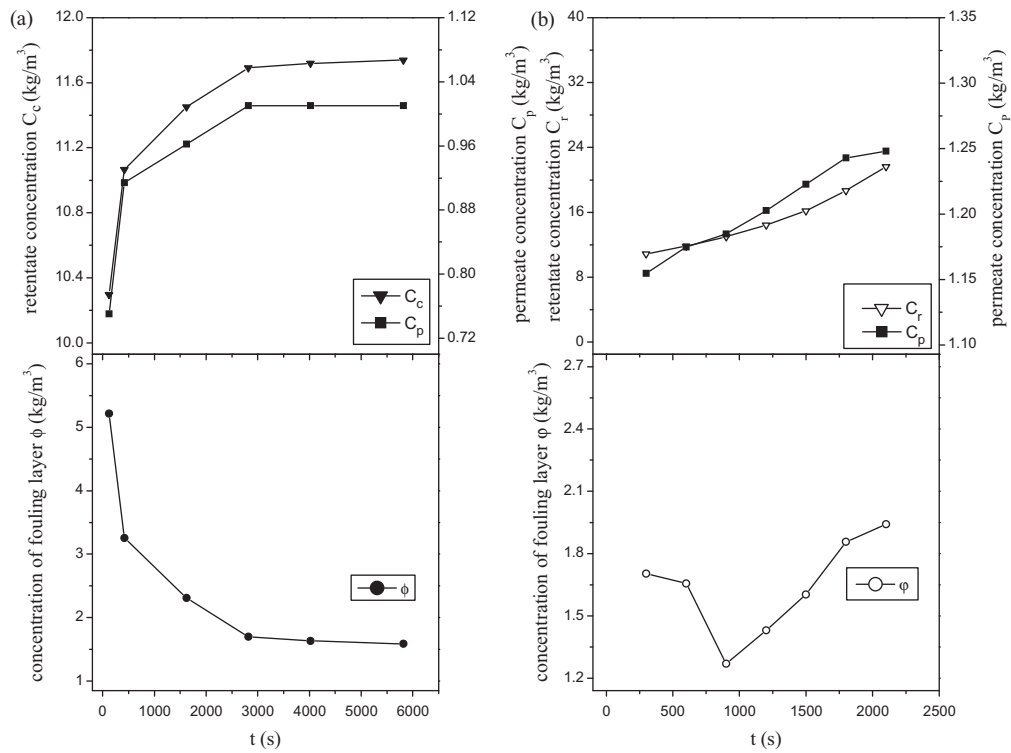


Fig. 3. The variations of SDS concentration in permeate and retentate solution as well as process parameters with time at feed concentration = 4 CMC, $TMP = 100$ kPa. (a) Retentate non-recycled cross-flow and (b) retentate recycled cross-flow.

as $R_m = 1/(\mu_0 \times slope)$, μ_0 is dynamic viscosity of pure water in 30 °C. The membrane hydrodynamic resistance is $2.64 \times 10^{12} \text{ m}^{-1}$.

Desired feed concentration solution was prepared in retentate non-recycled and recycled system respectively using deionized water and the solution would be placed for 1 h in order to form cadmium-micelles. After filling up feed tank, solution was pumped to cell and volumes of permeate were collected at desired times using measuring cylinder. The samples of permeate and retentate stream were also collected at desired times to analysis SDS concentration. The instantaneous permeate and retentate flow was measured by flowmeter at each time in order to calculate permeate flux. TMP was calculated as $TMP = (P_{in} + P_{out})/2$.

After each experiment, for recovering its permeability, membrane was washed thoroughly with the help of distilled water for 1 h, NaOH (0.5 mol/L) for 30 min, deionized water for 30 min at the pressure of 100 kPa.

3.4. Analysis

SDS concentration in permeate and retentate is determined by methylene blue spectrophotometric method [32] (ISO-7875-1-1996) with Shimadzu UV-2550 (P/N206-55501-93) spectrophotometer, Japan.

4. Results and discussion

4.1. Determination of specific fouling resistance

The special fouling resistance of each cross-flow types was obtained by fitting experimental data and using following expression, which was deformed from Eqs. (12) and (19). Retentate non-recycled system:

$$J_1^{-2} = \frac{\mu^2 R_m^2}{TMP^2} + \frac{2\alpha\mu}{TMP} \phi t = b + c\phi t \quad (20)$$

Retentate recycled system:

$$J_2^{-2} = \frac{\mu^2 R_m^2}{TMP^2} + \frac{2\alpha\mu}{TMP} \phi t = b' + c'\phi t \quad (21)$$

where the slope of J_1^{-2} versus ϕt plot gave the value of special fouling resistance. From each set of experiments (i.e., TMP and feed SDS concentration), slope of Eq. (20) was showed and the special fouling resistance was calculated as $\alpha = TMP \times slope / 2\mu$. Similarly, special fouling resistance in retentate recycled system was calculated by the same method by Eq. (21). Variations of α with different TMP and feed SDS concentration were showed in Table 1. Moreover, the specific fouling resistance was correlated with operating conditions [23] as: (i) Retentate non-recycled system:

$$\alpha = \alpha_0 (TMP)^{s1} \left(\frac{C_0^{SDS}}{C_0^{Cd}} \right)^{s2} \quad (22)$$

where C_0^{SDS} , C_0^{Cd} are identified as feed SDS and Cd concentration, respectively. Next, $\alpha_0 = 3.784 \times 10^7 \text{ m/kg}$, $s1 = 1.411$, $s2 = -1.767$.

(ii) Retentate recycled system:

$$\alpha = \alpha'_0 (TMP)^{s3} (C_0^{SDS} / C_0^{Cd})^{s4} \quad (23)$$

Next, $\alpha'_0 = 1.353 \times 10^{11} \text{ m/kg}$, $s3 = 0.547$, $s4 = -0.789$.

In Eqs. (22) and (23), the specific fouling resistance is directly proportional to TMP , and inversely proportional to the value of initial feed concentration. And the effects of TMP and initial feed concentration on permeate flux curve could be determined by Eqs. (20) and (21).

4.2. Determination of membrane hydrodynamic resistance

The method to calculate R_m has been introduced in Section 3.3. However, membrane hydrodynamic resistance also could be calculated by intercept of the straight-line Eqs. (20) and (21).

Table 1The results related to permeate flux decline in various TMP and feed SDS concentration at $C_0^{SDS} = 100$ mg/L.

(a) Retentate non-recycled cross-flow						
TMP (kPa)	C_0^{SDS} (CMC)	Flux model of retentate non-recycle cross-flow				
		$b \times 10^8$ (s ² /m ²)	$c \times 10^3$ (m s/kg)	r^2	$\alpha \times 10^{12}$ (m/kg)	$R_m \times 10^{12}$ (m ⁻¹)
60	4	3.019	1.993	0.956	0.075	1.70
	1	1.944	27.788	0.968	1.737	1.74
100	2	2.002	6.289	0.951	0.393	1.77
	4	2.020	2.398	0.974	0.150	1.78
150	4	1.819	2.884	0.936	0.270	2.53

(b) Retentate recycled cross-flow						
TMP (kPa)	C_0^{SDS} (CMC)	Flux model of retantate recycled cross-flow				
		$b' \times 10^8$ (s ² /m ²)	$c' \times 10^3$ (m s/kg)	r^2	$\alpha \times 10^{12}$ (m/kg)	$R_m \times 10^{12}$ (m ⁻¹)
60	4	2.995	41.625	0.942	1.561	1.68
	1	1.827	106.560	0.979	6.660	1.69
100	2	2.016	43.943	0.974	2.746	1.77
	4	1.954	35.675	0.990	2.230	1.75
150	4	1.806	27.322	0.935	2.561	2.52

Note: Membrane hydrodynamic resistance R_m is 2.64×10^{12} (m⁻¹) measured by pure water (Section 3.3).

From each set of experiments (i.e., TMP and feed SDS concentration), membrane hydrodynamic resistance was calculated as $R_m = TMP \times (\text{intercept})^{1/2} / \mu$ and values in different initial conditions were shown in Table 1.

Furthermore, R_m calculated by the method described in Section 3.3 and the method inferred from intercept of model (i.e., Eqs. (20) and (21)), were difference. And R_m in various initial conditions used the latter method were also not the same. Furukawa et al. [33] has

reported membrane hydrodynamic resistance was different among UF membrane in different TMP . Observed Table 1, R_m calculated by method described in Section 3.3 was higher than by method inferred from the intercept of model. It increased gradually with increase of TMP and kept a constant largely with increase of feed SDS concentration. That may be because each membrane has its own range of TMP , and TMP may change hydrodynamic resistance characteristics of membrane.

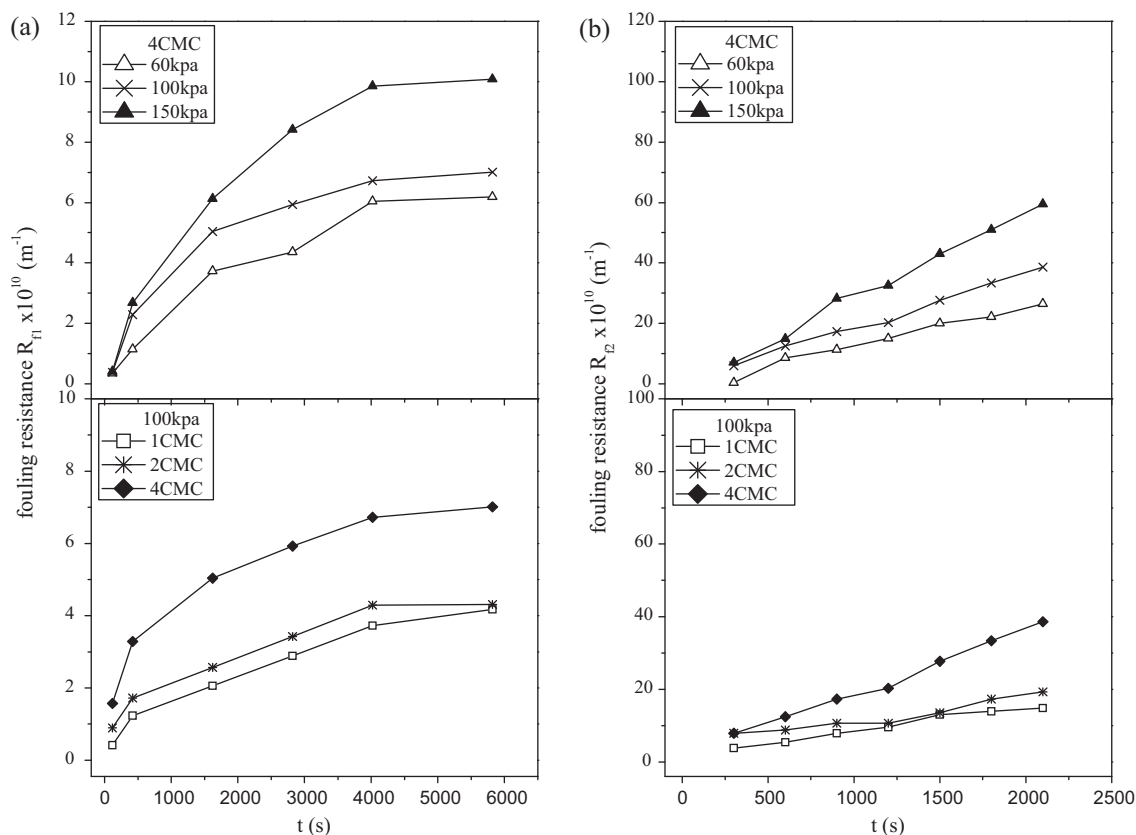


Fig. 4. The variations of fouling resistance with time as the function of feed SDS concentration and TMP . (a) Retentate non-recycled cross-flow and (b) retentate recycled cross-flow.

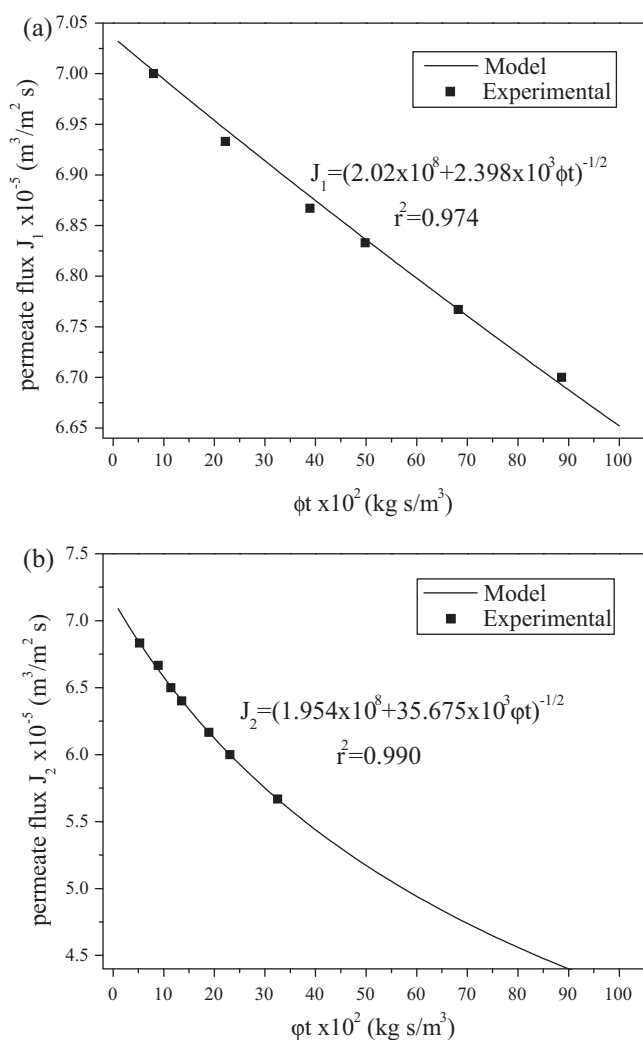


Fig. 5. Comparison between the experimental and model permeate flux at feed concentration of 4 CMC and TMP of 100 kPa. (a) Retentate non-recycled cross-flow and (b) retentate recycled cross-flow.

4.3. Determination of concentration of fouling layer ϕ and φ

In the process of MEUF, variables needed to be considered, including rate of reflux, concentration of permeate and retentate. Experimental parameters ϕ and φ integrated from these variables and represented the concentration of fouling layer. They could be calculated by the definition introduced at Section 2.2. However, ϕ could be seen as a constant after a certain time and φ could be predicted with the help of volume reduction factor VRF [33] that were mentioned in the next Section 4.3.2.

4.3.1. Prediction of ϕ in retentate non-recycled system

In retentate non-recycled system, the rate of concentration could be controlled by retentate back pressure valve, and then a certain condensed degree of feed f was determined. Variations of SDS concentration in permeate and retentate was shown in Fig. 3(a). It was observed that SDS concentration in permeate and retentate rapidly increased at initial 2800 s and tended to unchanged basically. Therefore, the value of ϕ could be seen as a constant after 2800 s which was shown in Fig. 3(a). Therefore, concentration of fouling layer could be seen as a constant after 2800 s in retentate non-recycled system.

4.3.2. Prediction of φ in retentate recycled system

In retentate recycled system, studies have been reported SDS concentration in permeate was 1 CMC [21]. However, steady permeate surfactant concentration in the present study showed in Fig. 3(b) kept at 0.4–0.6 CMC. This may be due to solute was filtered by a dense fouling layer besides membrane and this process improved the rejection of membrane filtration.

The rate of recycled was controlled by retentate back pressure valve, and return rate w was determined by volume of solution remained in feed tank. Fig. 3(b) depicted the trend of SDS concentration in permeate and retentate. Permeate SDS concentration tended to be the same after 1800 s and retentate SDS concentration rapidly increased with filtration. Fig. 3(b) showed the variations of concentration of fouling layer φ with time. Due to permeate concentration tended to be a constant, according to the definition of φ , retentate concentration C_r and volume became the main affecting factors to φ after 1800 s. Furukawa et al. [33] used volume reduction factor VRF to predict retentate concentration C_r and defined $VRF = C_r/C_0 = V_0/(V_0 - V)$, then C_r and φ could be determined by VRF .

4.4. Modeling of fouling resistance

4.4.1. Fouling resistance in retentate non-recycled system

Experimental fouling resistance was determined from experimental permeate flux by using Eq. (1). Fig. 4(a) was mapped for better illustrate the effects of three typical TMP of 60 kPa, 100 kPa, 150 kPa and feed SDS concentrations of 1 CMC, 2 CMC, 4 CMC to fouling resistance. It gradually increased and finally tended to be a constant. That was due to a balance between the life force and the drag force, gradually built up with time [34]. It was evident from the figure that fouling resistance was greater for higher TMP because of larger dense of fouling layer over the membrane surface. De et al. [26] showed smaller porosity and larger dense for higher TMP . From Eq. (7), it also showed that smaller porosity means greater specific fouling resistance and larger dense. On the other hand, fouling resistance was larger for higher feed concentration at same TMP . Although higher feed concentration made smaller specific fouling resistance (Section 4.1), the number of micelles is greater, leading to more number of micelles attached to the membrane surface and increased the thickness of fouling layer. Studies have reported that the higher feed concentration above the CMC, the greater fouling resistance [22,35,36].

4.4.2. Fouling resistance in retentate recycled system

With various operational conditions, similar effects were shown in Fig. 4(b) that fouling resistance was greater for higher TMP and higher feed concentration. That may due to retentate solution was concentrated constantly and the concentration of it increased with time.

4.5. Modeling of permeate flux decline

Comprehensive analysis concerning flux decline versus ϕt (or φt) was carried out by evaluating of the results, feed SDS concentration of 4 CMC and TMP of 100 kPa, as shown in Fig. 5. Flux decline models of retentate non-recycled and recycled system presented admirably good correlations in terms of r^2 values. The results of it in various operational conditions were shown in Table 1.

4.5.1. Modeling of flux decline in retentate non-recycled system

Fig. 6(a) shows permeate flux decline with time in retentate non-recycled system at various TMP and three different feed SDS concentrations. With operational conditions, permeate flux decline rapidly at initial 2800 s and finally tended to be the same. This may due to fouling resistance gradually formed at membrane surface and achieved a balance between newly formed and dragged away

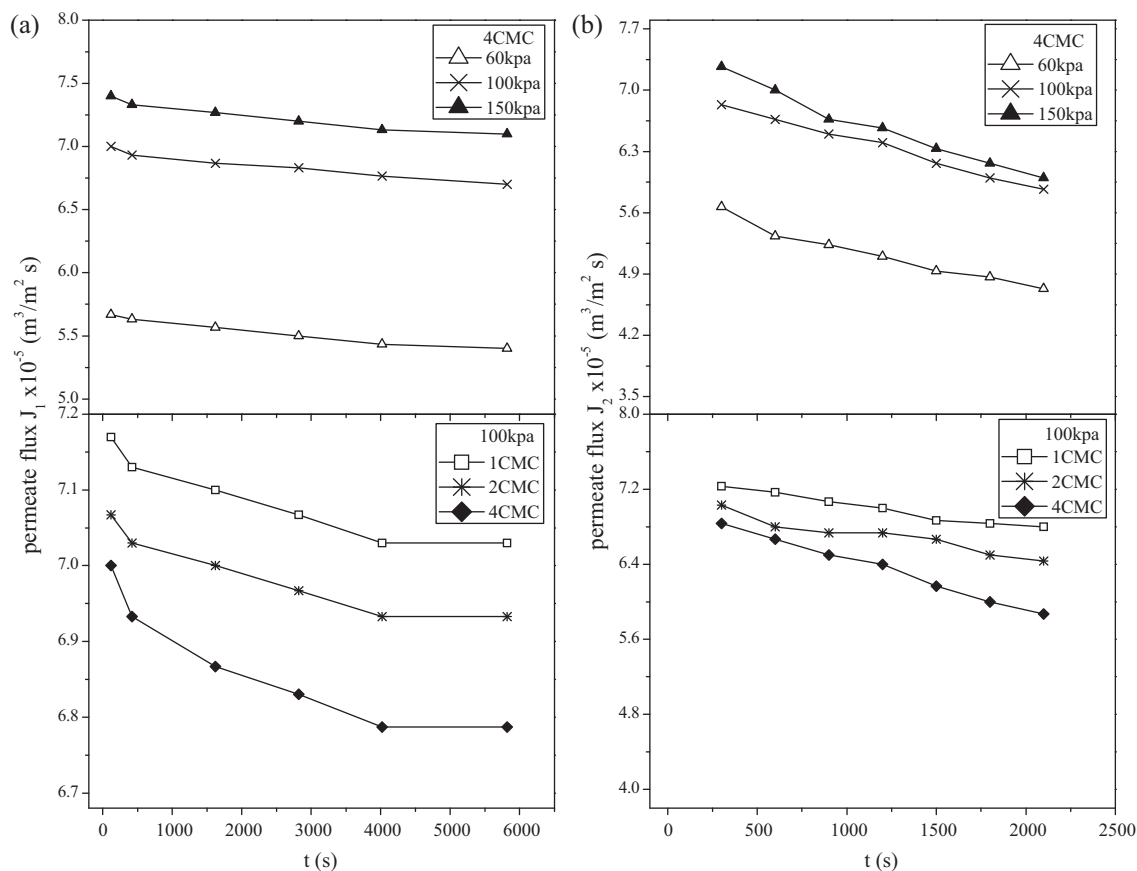


Fig. 6. The variations of permeate flux with time as the function of feed SDS concentration and TMP . (a) Retentate non-recycled cross-flow and (b) retentate recycled cross-flow.

by shear force after 2800 s. It was evident from Fig. 6(a) that permeate flux was lower for higher feed concentration at a certain TMP because of greater fouling resistance. On the other hand, at any point of operating time, permeate flux was higher for higher TMP .

Total transport resistance has two parts: fouling resistance, $10^{10} \text{ (m}^{-1}\text{)}$ shown in Fig. 4(a) and membrane resistance, $10^{12} \text{ (m}^{-1}\text{)}$ shown in Table 1. Therefore, in Section 4.1, although s_1 was greater than 1, fouling resistance depends on pressure to greater than the first power, the main factor to affect total transport resistance is membrane resistance. Therefore, with the help of Eq. (1), this result in a flux that increases with increasing pressure was a normal phenomenon shown in Fig. 6(a). Studies had been researched that permeate flux was lower for higher TMP because of greater fouling resistance [22,33] and permeate flux was higher for higher TMP because of larger driving force [23,29]. For these diametrically opposite conclusions, it also could be interpreted with the help of Eq. (1). In summary, the effect of TMP on permeate flux depended on which was the dominant factor, driving force or total transport resistance during different membranes and filtration process.

4.5.2. Modeling of flux decline in retentate recycled system

Permeate flux was lower for higher feed concentration due to greater micelles on membrane surface, shown in Fig. 6(b). And permeate flux was higher for higher TMP . Although fouling resistance was also higher for higher TMP , the increment of fouling resistance was less than TMP because s_3 was lower than 1 (Section 4.1). Therefore, with the help of Eq. (1), the overall result in permeate flux that increases with increasing TMP .

5. Conclusions

The present study focused on establishing a suitable fouling resistance model and permeate flux model of two types cross-flow MEUF by theoretical derivation and experimental verification. Based on material balance of cross-flow and hydrodynamic type of MEUF, model of permeate flux versus concentration of fouling layer and time was developed instead of traditional fouling resistance model that permeate flux only with the relationship of time. Models showed excellent accuracy to predict permeate flux through correlation r^2 from 0.935 to 0.990. It could be used to calculate specific fouling resistance and membrane hydrodynamic resistance intuitively through constant parameters b , c or b' , c' and concentration of fouling layer on membrane surface through parameters ϕ , φ . In addition, the methods of modeling could extend to other filtration through identify fluid type (laminar flow or turbulent flow) and material balance (batch filtration or continuous filtration) of the filtering process.

Acknowledgments

This study was financially supported by the National Natural Science Foundation of China (50608028, 51178172, 50978088, 51008121, 51039001), the Program for New Century Excellent Talents in University from the Ministry of Education of China (NCET-08-180, NCET-08-0181), the Xiangjiang Water Environmental Pollution Control Project Subjected to the National Key Science and Technology Project for Water Environmental Pollution Control (2009ZX07212-001-02 and 2009ZX07212-001-06), the Hunan Key

Scientific Research Project (2009FJ1010), and the Hunan Provincial Natural Science Foundation of China (10JJ7005).

References

- [1] F. Luo, G.M. Zeng, J.H. Huang, et al., Effect of groups difference in surfactant on solubilization of aqueous phenol using MEUF, *J. Hazard. Mater.* 173 (2010) 455–461.
- [2] J. Iqbal, H. Kim, J. Yang, et al., Removal of arsenic from groundwater by micellar enhanced ultrafiltration (MEUF), *Chemosphere* 66 (2007) 970–976.
- [3] L. Ghezzi, B.H. Robinson, F. Secco, et al., Removal and recovery of palladium(II) ions from water using micellar-enhanced ultrafiltration with a cationic surfactant, *Colloids Surf. A: Physicochem. Eng. Aspects* 329 (2008) 12–17.
- [4] J.H. Huang, G.M. Zeng, Y.Y. Fang, et al., Removal of cadmium ions using micellar-enhanced ultrafiltration with mixed anionic-nonionic surfactants, *J. Membr. Sci.* 326 (2009) 303–309.
- [5] V.D. Karate, K.V. Marathe, Simultaneous removal of nickel and cobalt from aqueous stream by cross flow micellar enhanced ultrafiltration, *J. Hazard. Mater.* 157 (2008) 464–471.
- [6] K. Baek, Removal characteristics of anionic metals by micellar-enhanced ultrafiltration, *J. Hazard. Mater.* 99 (2003) 303–311.
- [7] Y.K. Bayhan, B. Keskinler, A. Cakici, et al., Removal of divalent metal mixtures from water by *Saccharomyces cerevisiae* using crossflow microfiltration, *Water Res.* 35 (2001) 2191–2200.
- [8] M.K. Purkait, S. DasGupta, S. De, Simultaneous separation of two oxyanions from their mixture using micellar enhanced ultrafiltration, *Sep. Sci. Technol.* 40 (2005) 1439–1460.
- [9] R.S. Juang, Y.Y. Xu, C.L. Chen, Separation and removal of metal ions from dilute solutions using micellar-enhanced ultrafiltration, *J. Membr. Sci.* 218 (2003) 257–267.
- [10] C. Das, P. Maity, S. DasGupta, et al., Separation of cation/anion mixture using micellar-enhanced ultrafiltration in a mixed micellar system, *Chem. Eng. J.* 144 (2008) 35–41.
- [11] S. Akita, L.P. Castillo, S. Nii, et al., Separation of Co(II)/Ni(II) via micellar-enhanced ultrafiltration using organophosphorus acid extractant solubilized by nonionic surfactant, *J. Membr. Sci.* 162 (1999) 111–117.
- [12] S. Ripperger, J. Altmann, Crossflow microfiltration state of art, *Sep. Purif. Technol.* 26 (2002) 19–31.
- [13] H. Kim, K. Baek, J. Lee, et al., Comparison of separation methods of heavy metal from surfactant micellar solutions for the recovery of surfactant, *Desalination* 191 (2006) 186–192.
- [14] K. Baek, B.K. Kim, J.W. Yang, Application of micellar enhanced ultrafiltration for nutrients removal, *Desalination* 156 (2003) 137–144.
- [15] K. Baek, J.W. Yang, Cross-flow micellar-enhanced ultrafiltration for removal of nitrate and chromate: competitive binding, *J. Hazard. Mater.* B108 (2004) 119–123.
- [16] J.S. Yang, K. Baek, J.W. Yang, Crossflow ultrafiltration of surfactant solutions, *Desalination* 184 (2005) 385–394.
- [17] A. Witek, A. Koltuniewicz, B. Kurczewski, et al., Simultaneous removal of phenols and Cr^{3+} using micellar-enhanced ultrafiltration process, *Desalination* 191 (2006) 111–116.
- [18] S.K. Misra, A.K. Mahatele, S.C. Tripathi, et al., Studies on the simultaneous removal of dissolved DBP and TBP as well as uranyl ions from aqueous solutions by using Micellar-Enhanced Ultrafiltration Technique, *Hydrometallurgy* 96 (2009) 47–51.
- [19] L. Gzara, M. Dhahbi, Removal of chromate anions by micellar-enhanced ultrafiltration using cationic surfactants, *Desalination* 137 (2001) 241–250.
- [20] M. Mulder, *Basic Principles of Membrane Technology*, 2nd ed., Kluwer Academic Publishers, Netherlands, 1996.
- [21] C. Das, S. DasGupta, S. De, Prediction of permeate flux and counterion binding during cross-flow micellar-enhanced ultrafiltration, *Colloids Surf. A: Physicochem. Eng. Aspects* 318 (2008) 125–133.
- [22] U. Danis, C. Aydinler, Investigation of process performance and fouling mechanisms in micellar-enhanced ultrafiltration of nickel-contaminated waters, *J. Hazard. Mater.* 162 (2009) 577–587.
- [23] M.K. Purkait, S. DasGupta, S. De, Resistance in series model for micellar enhanced ultrafiltration of eosin dye, *J. Colloid Interface Sci.* 270 (2004) 496–506.
- [24] B. Rahmanian, M. Pakizeh, M. Esfandiyari, et al., Fuzzy modeling and simulation for lead removal using micellar-enhanced ultrafiltration (MEUF), *J. Hazard. Mater.* 192 (2011) 585–592.
- [25] E. Turano, S. Curcio, M.G. De Paola, et al., An integrated centrifugation-ultrafiltration system in the treatment of olive mill wastewater, *J. Membr. Sci.* 209 (2002) 519–531.
- [26] S. De, P.K. Bhattacharya, Modeling of ultrafiltration process for a two-component aqueous solution of low and high (gel-forming) molecular weight solutes, *J. Membr. Sci.* 136 (1997) 57–69.
- [27] M. Ousman, M. Bannasar, Determination of various hydraulic resistances during cross-flow filtration of a starch grain suspension through inorganic membranes, *J. Membr. Sci.* 105 (1995) 1–21.
- [28] M.J. Rosen, *Surfactants and Interfacial Phenomena*, 3rd ed., John Wiley and Sons, Inc., Hoboken, 2004.
- [29] C.J. Geankoplis, *Transport Processes and Unit Operations*, 3rd ed., Prentice-Hall International, London, 1993.
- [30] R.G. Grisley, *Transport Phenomena and Unit Operations*, John Wiley and Sons, Inc, NY, 2002.
- [31] M. Lindberg, A. Grslund, The position of the cell penetrating peptide penetratin in SDS micelles determined by NMR, *FEBS Lett.* 497 (2001) 39–44.
- [32] Y.Y. Fang, G.M. Zeng, J.H. Huang, et al., Micellar-enhanced ultrafiltration of cadmium ions with anionic/nonionic surfactants, *J. Membr. Sci.* 320 (2008) 514–519.
- [33] T. Furukawa, K. Kokubo, K. Nakamura, et al., Modeling of the permeate flux decline during MF and UF cross-flow filtration of soy sauce lees, *J. Membr. Sci.* 322 (2008) 491–502.
- [34] J. Altmann, S. Ripperger, Particle deposition and layer formation at the cross-flow microfiltration, *J. Membr. Sci.* 124 (1997) 119–128.
- [35] X. Li, G.M. Zeng, J.H. Huang, et al., Simultaneous removal of cadmium ions and phenol with MEUF using SDS and mixed surfactants, *Desalination* 276 (2011) 136–141.
- [36] R.S. Juang, S.H. Lin, L.C. Peng, Flux decline analysis in micellar-enhanced ultrafiltration of synthetic waste solutions for metal removal, *Chem. Eng. J.* 161 (2010) 19–26.